Multicompartment Core Micelles of Triblock Terpolymers in Organic Media

Felix Schacher,*,† Andreas Walther,‡ Markus Ruppel,§ Markus Drechsler,† and Axel H. E. Müller*,†

Makromolekulare Chemie II and Zentrum für Kolloide and Grenzflächen, Universität Bayreuth, 95440 Bayreuth, Germany, Department of Applied Physics, Helsinki University of Technology, FIN-02015 TKK, Helsinki, Finland, and Oak Ridge National Laboratory, Oak Ridge, Tennessee 37831

Received February 3, 2009; Revised Manuscript Received March 18, 2009

ABSTRACT: The formation of multicompartment micelles featuring a "spheres on sphere" core morphology in acetone as a selective solvent is presented. The polymers investigated are ABC triblock terpolymers, polybutadiene-*b*-poly(2-vinyl pyridine)-*b*-poly(*tert*-butyl methacrylate) (BVT), which were synthesized via living sequential anionic polymerization in THF. Two polymers with different block lengths of the methacrylate moiety were studied with respect to the formation of multicompartmental aggregates. The micelles were analyzed by static and dynamic light scattering as well as by transmission electron microscopy. Cross-linking of the polybutadiene compartment could be accomplished via two different methods, "cold vulcanization" and with photopolymerization after the addition of a multifunctional acrylate. In both cases, the multicompartmental character of the micellar core is fully preserved, and the micelles could be transformed into core-stabilized nanoparticles. The successful cross-linking of the polybutadiene core is indicated by ^{1}H NMR and by the transfer of the aggregates into nonselective solvents such as THF or dioxane.

Introduction

Multicompartment micelles can combine several properties or functionalities in close proximity and are therefore promising candidates for a new class of nanomaterials. Different research groups have worked to develop diverse strategies for the preparation of such micelles in aqueous media. The term "multicompartment micelles", or more precisely, "multicompartment core micelles", stands for self-assembled aggregates of block copolymers with cores that are further subdivided. The principal concept was introduced by Ringsdorf[1] around 10 years ago, and a recent review reports on the progress within this field of research.[2] Those structures are of great interest when it comes to the simulation or understanding of biological systems where different functionalities in close proximity are necessary to perform distinct biological functions.[3] Multicompartment micelles are very promising candidates for drug-delivery applications, especially for entrapment or release of hydrophobic species in different media. Different groups investigated the selective solubilization in multicompartmental micellar cores.[4−7] Hillmyer et al. demonstrated the possibility of storing two different dyes in two segregated compartments of such a multicompartmental structure in various aqueous micellar solutions.[8]

Complex structures have been prepared from ABC triblock terpolymers in solution.[9−11] In contrast with the large number of reports on micellar aggregates from diblock copolymers or the structures of ABC triblock terpolymers in the bulk, the number of contributions on triblock terpolymer micelles in selective solvents is still limited.[12−16] In particular, the formation and the control of the stability of such systems are not yet very well studied and understood. Most of the current approaches toward multicompartmental architectures are based on the mutual incompatibility of fluorocarbon and hydrocarbon segments of self-assembled systems in aqueous media.[3,8,17,18] One very recent example employs an ABCBA pentablock terpolymer of poly(ethylene oxide) (PEO), poly(γ-benzyl-L-glutamate) (PBLG), and poly(perfluoroether) (PFPE) in aqueous solution.[19] Complex polymer architectures may also lead to the formation of multicompartmental structures. Lodge et al. reported on ABC miktoarm star terpolymers, poly(ethyl ethylene)-*b*-poly(ethylene oxide)-*b*-poly(perfluoropropylene oxide).[20,21] The star architecture can suppress the formation of concentric microphase domains. This has also been demonstrated by Hillmyer et al. for polyester-containing ABC miktoarm star polymers with arms of PEO, poly(ethyl ethylene), and poly(γ-methyl-ε-caprolactone).[22] Additionally, charged polymer segments may induce a further compartmentalization of either core or corona as well, as shown by Yan et al.[23] Theoretical aspects of the micelle formation from ABC terpolymers as model systems depending on block sequence, architecture, and molecular weight have been addressed[24−27] and have broadened the scope and interest of multicompartment architectures.

In this article, we present the formation of multicompartment core micelles in acetone solution from polybutadiene-*b*-poly(2-vinyl pyridine)-*b*-poly(*tert*-butyl methacrylate) (BVT) triblock terpolymers and their stabilization by cross-linking. The polymers were synthesized via sequential anionic polymerization and exhibit a very narrow molecular weight distribution (PDI < 1.04). The formed aggregates have been investigated by transmission electron microscopy (TEM), cryogenic transmission electron microscopy (cryo-TEM), and light scattering methods. The micelles are stable with respect to the cross-linking of the double bonds of the polybutadiene compartment. Cross-linking was carried out via either "cold vulcanization" with S_2Cl_2 or through UV-photopolymerization in the presence of a tetrafunctional acrylate. The effect of the amount of cross-linking agent, the reaction time, or both on the size and the shape of the generated nanostructures was also studied. After the cross-linking reactions were performed in solution, the micelles were again subjected to electron microscopy and light scattering analysis. The success of the cross-linking was proven by the

* Corresponding authors. E-mail: felix.schacher@uni-bayreuth.de; axel.mueller@uni-bayreuth.de.
† Universität Bayreuth.
‡ Helsinki University of Technology.
§ Oak Ridge National Laboratory.

10.1021/ma9002424 CCC: $40.75
Published on Web 04/10/2009

transfer of the micellar aggregates into THF, a nonselective solvent for all three blocks. In contrast with other works within this field, the employed building blocks here are rather simple and consist of standard, easy-to-handle monomers. It is noteworthy that in all cases, only one single population of aggregates was found, and the micellar solutions are stable over several months, both before and after the cross-linking steps.

Experimental Part

Materials. *sec*-Butyllithium, S_2Cl_2, and pentaerythrol tetraacrylate (Aldrich) were used without further purification. Butadiene (Messer-Griesheim) was passed through columns filled with molecular sieves (4 Å) and basic aluminum oxide. Afterwards, it was condensed into a glass reactor and stored over dibutylmagnesium. 2-Vinyl pyridine (Fluka) was degassed and stirred with CaH_2 overnight. The monomer was condensed on a high vacuum line into a round-bottomed flask containing 2 mL of triethylaluminum (solution in hexane, Aldrich) per 10 mL of 2-vinyl pyridine. The resulting yellow solution was stirred for 2 h. Subsequently, the calculated amount of monomer was condensed into a previously weighed glass ampule and stored in liquid nitrogen until use. *tert*-Butyl methacrylate (BASF) was first degassed by three freeze−thaw cycles on a high vacuum line. Then, trioctylaluminum (solution in hexane, Aldrich) was added until a slight yellow color of the resulting mixture persisted. The solution was stirred for 1 h, and the calculated amount of monomer was condensed into a previously weighed glass ampule and stored in liquid nitrogen until use. THF (Fluka) was distilled from CaH_2 and Na/K alloy. 1,1-Diphenylethylene was distilled from *sec*-butyllithium under reduced pressure. The solvents for the preparation of the micellar solutions were purchased in p.a. grade and were used as delivered.

Synthesis. *Sequential Living Anionic Polymerization in THF.* The linear BVT triblock terpolymers were synthesized via sequential living anionic polymerization in THF at low temperatures using *sec*-butyllithium as initiator. Under these conditions, mainly 1,2-polybutadiene (86%, confirmed by ^{1}H NMR measurements) is generated. After the polymerization of the P2VP block, 1,1-diphenylethylene was added to end-cap the living ends of the anions. In this way, crossover steps and transfer reactions due to too high nucleophilicity upon the addition of the third monomer could be suppressed.[28,29] During the polymerization of the P*t*BMA block, samples were taken from the reactor after different polymerization times and were precipitated into degassed methanol. The number-average molecular weight of the polybutadiene precursor and the molecular weight distributions of the triblock terpolymers were determined by gel permeation chromatography. In the case of the polybutadiene precursor, MALDI-ToF mass spectrometry was employed to receive the absolute molecular weight. All of the polymers exhibit narrow molecular weight distributions characterized by a polydispersity index between 1.02 and 1.03. Additionally, ^{1}H NMR spectra were recorded, and the molecular weights of the P2VP and P*t*BMA blocks were calculated using the triblock terpolymer composition determined by NMR and GPC. The GPC curves for $B_{800}V_{190}T_{380}$, $B_{800}V_{190}T_{550}$, and the corresponding precursors are shown in Figure 1, and the molecular characteristics are shown in Table 1. Both polymers mentioned showed a lamellar (ll) morphology in the bulk state with characteristic long periods of 78 ($B_{800}V_{190}T_{380}$) and 85 nm ($B_{800}V_{190}T_{550}$).

Cross-Linking via Cold Vulcanization with S_2Cl_2. To a micellar solution of 1 mg/mL $B_{800}V_{190}T_{550}$ in acetone was added 1, 2, or 5 equiv (functional groups of cross-linking agent with respect to the amount of remaining double bonds from the first block of the terpolymer) of S_2Cl_2. Afterwards, the dispersion was stirred for around 2 h. The unreacted S_2Cl_2 was removed through dialysis against acetone (dialysis tube, MWCO = 10 000 g/mol).

Cross-Linking with Pentaerythrol Tetraacrylate. To a micellar solution of 1 mg/mL $B_{800}V_{190}T_{550}$ in acetone was added 0.5, 1, or 2 equiv (functional groups of cross-linking agent with respect to the amount of remaining double bonds from the first block of the terpolymer) of multifunctional acrylate. Afterward, the dispersion was stirred for around 2 h to equilibrate. Cross-linking was performed through irradiation of the dispersion with a UV lamp (Hoenle VG-UVAHAND 250 GS equipped with a glass filter, cutoff at 300 nm wavelength to avoid depolymerizing the methacrylic compartment). The unreacted cross-linking agent was removed through dialysis against acetone (dialysis tube, MWCO = 10 000 g/mol).

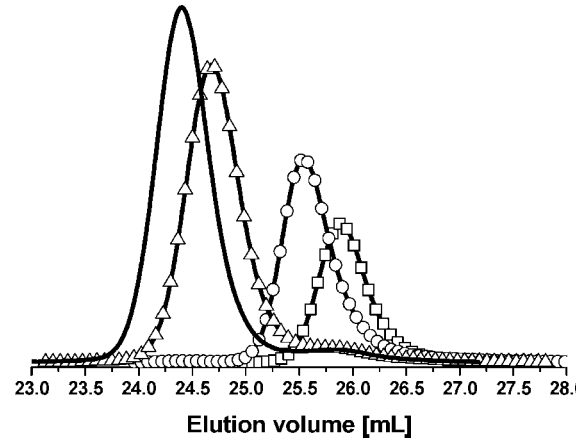

Figure 1. SEC elution traces of B_{800} (-□-), $B_{800}V_{190}$ (-○-), and the two triblock terpolymers $B_{800}V_{190}T_{380}$ (-△-) and $B_{800}V_{190}T_{550}$ (—).

Table 1. Molecular Characteristics of the BVT Block Terpolymers Employed

composition[a]	composition[b]	$10^{-3}M_w$[c]	polydispersity[d]
$B_{37}V_{17}T_{46}^{117}$	$B_{800}V_{190}T_{380}$	117	1.03
$B_{30}V_{14}T_{56}^{141}$	$B_{800}V_{190}T_{550}$	141	1.02

[a] Subscripts are weight fractions; the superscript is the overall molecular weight in kg/mol. [b] Subscripts are degrees of polymerization. [c] Determined by combination of MALDI-TOF MS and ^{1}H NMR. [d] Determined via THF-SEC calibrated with 1,4-polybutadiene standards.

Characterization. Gel permeation chromatography measurements were performed on a set of 30 cm SDV-gel columns of 5 mm particle size having a pore size of 10^5, 10^4, 10^3, and 10^2 Å with refractive index and UV (λ = 254 nm) detection. GPC was measured at an elution rate of 1 mL/min with THF as eluent.

^{1}H NMR spectra were recorded on a Bruker 250 AC spectrometer using either $CDCl_3$ or THF as solvent and tetramethylsilane (TMS) as internal standard.

Dynamic light scattering (DLS) measurements were performed in sealed cylindrical scattering cells (d = 10 mm) at five scattering angles of 30, 60, 90, 120, and 150° on ALV DLS/SLS-SP 5022F equipment consisting of an ALV-SP 125 laser goniometer with an ALV 5000/E correlator and a He−Ne laser with the wavelength λ = 632.8 nm. The CONTIN algorithm was applied to analyze the obtained correlation functions. Apparent hydrodynamic radii were calculated according to the Stokes−Einstein equation. Prior to the light scattering measurements, the sample dispersions were filtered using Millipore PTFE filters with a pore size of 1 μm. The polydispersities were determined from unimodal peaks via the cumulant analysis.

Static Light Scattering. Micellar solutions of the polymers were prepared in the concentration range between 0.1 and 1 g/L. Static light scattering measurements were carried out on a Sofica goniometer with a He−Ne laser (λ = 632.8 nm) at RT. Prior to the measurements, sample dispersions were filtered through Millipore PTFE filters of pore size 1 μm. A Zimm plot was used to evaluate the data. A diffraction refractometer DnDC2010/620 (PSS) was used to measure refractive index increment, dn/dc (0.166 L/mol for $B_{800}V_{190}T_{380}$ and 0.148 for $B_{800}V_{190}T_{550}$), of the polymer micellar solution at λ = 620 nm.

Transmission Electron Microscopy. TEM images were taken with a Zeiss CEM902 EFTEM electron microscope operated at 80 kV or a Zeiss EM922 OMEGA EFTEM electron microscope operated at 200 kV. Both machines are equipped with an in-column energy

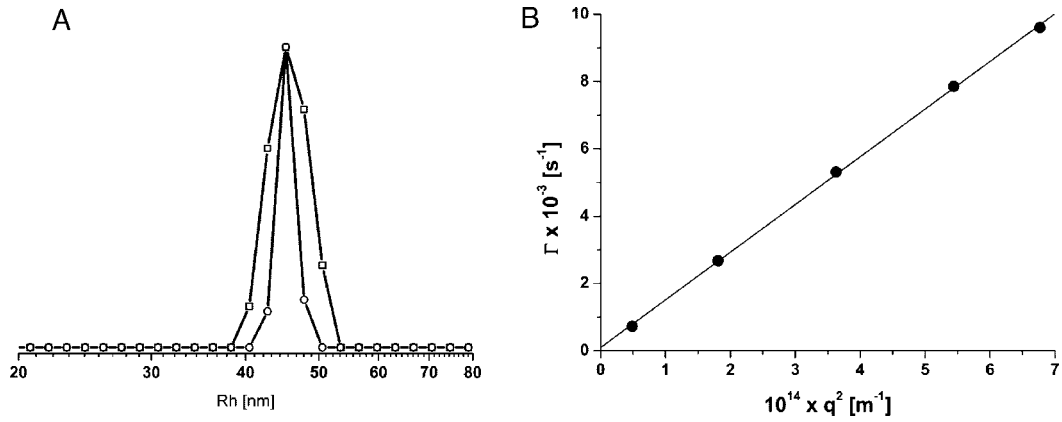

Figure 2. (A) CONTIN plots (intensity weighted) for $B_{800}V_{190}T_{380}$ (gray line, $\langle R_h \rangle_z = 43$ nm) and $B_{800}V_{190}T_{550}$ (black line, $\langle R_h \rangle_z = 44$ nm) at $\theta = 90°$ in acetone ($c = 1$ g/L). (B) Γ versus q^2 for $B_{800}V_{190}T_{550}$.

filter. Samples were prepared through deposition of a drop of micellar solution (concentration always 0.1 g/L) on the TEM grid (gold, 400 mesh). Afterwards, the remaining solvent was removed with a filter paper.

Cryogenic Transmission Electron Microscopy. A drop of the sample solution ($c \approx 0.5$ wt %, solvent being either THF or dioxane) was placed on a lacey carbon-coated copper TEM grid (200 mesh, Science Services, München, Germany) where most of the liquid was removed with blotting paper, leaving a thin film stretched over the grid holes. The specimens were shock vitrified by rapid immersion into liquid nitrogen in a temperature-controlled freezing unit (Zeiss Cryobox, Zeiss NTS GmbH, Oberkochen, Germany) and cooled to approximately 90 K. The temperature was monitored and kept constant in the chamber during all of the preparation steps. After freezing the specimens, they were inserted into a cryo-transfer holder (CT3500, Gatan, München, Germany) and transferred to a Zeiss EM922 OMEGA EFTEM instrument. Examinations were carried out at temperatures around 90 K. The transmission electron microscope was operated at an acceleration voltage of 200 kV. Zero-loss filtered images ($\Delta E = 0$ eV) were taken under reduced dose conditions (100−1000 e/nm^2). All images were registered digitally by a bottom-mounted CCD camera system (Ultrascan 1000, Gatan), combined, and processed with a digital imaging processing system (Gatan Digital Micrograph 3.9 for GMS 1.4).

Matrix-Assisted Laser Desorption Ionization Time-of-Flight Mass Spectrometry. MALDI-ToF MS analysis was performed on a Bruker Reflex III apparatus equipped with a 337 nm N_2 laser in the linear mode and 20 kV acceleration voltage. Sodium trifluoroacetate (NaTFA, Fluka, 99.5%) was used as salt to induce ion formation. We prepared samples from THF solution by mixing matrix (20 g/L) and the sample (1 mg) in a ratio of 10:1. The number-average molecular weight, M_n, of the sample was determined in the linear mode.

Results and Discussion

Synthesis of BVT Block Terpolymers. The two polymers shown in Table 1, $B_{800}V_{190}T_{380}$ and $B_{800}V_{190}T_{550}$, were used for the investigations in this work. The indices denote the degree of polymerization of the corresponding block. These are just two out of a series of several polymers with constant length ratio of first to second block and increasing poly(*tert*-butyl methacrylate) (P*t*BMA) content. They both display a very low polydispersity. The overall molecular weight was determined by a combination of MALDI-ToF mass spectra of the polybutadiene (PB) precursor and ^{1}H NMR spectra of the block copolymer. First, the molecular weight of the polybutadiene precursor was determined via MALDI-ToF mass spectrometry; then, the integrals of characteristic signals in the NMR spectra of the two other blocks were used for the calculation of the corresponding block lengths.The SEC elution traces in THF for the PB precursor, the PB-*b*-P2VP precursor, and the two BVT triblock terpolymers are shown in Figure 1.

Table 2. Solution Characteristics of the BVT Terpolymers in Acetone

R_h (nm)[a]	PDI[b]	R_g (nm)[c]	R_g/R_h	N_{agg}[c]	$10^6 A_2$ (mol mL/g^2)[e,c]
43	0.022	34	0.76	203 ± 3[d]	−5.13
44	0.016	36	0.82	174 ± 3[d]	−4.82

[a] Determined by DLS at $c = 1$ g/L. [b] Deviation determined by cumulant analysis at 90°. [c] Determined by SLS. [d] Determined via a linear fit of the extrapolated values for $c \rightarrow 0$ and $\Theta \rightarrow 0$ in Figure 3. [e] Second virial coefficient, determined via SLS.

To induce micelle formation, the polymers need to be dissolved in a selective solvent. Acetone is known to be a nonsolvent for polybutadiene.[30] The micelle formation was investigated in a concentration regime from 0.05 to 5 g/L. When dispersed in acetone at room temperature, the BVT triblock terpolymers immediately form aggregates, indicated by a turbid dispersion. This process is quite fast; the polymers are completely dissolved after 5 min. The so-formed micelles were expected to consist of a B core and a corona consisting of V and T.

Dynamic Light Scattering. DLS was used to assess the average hydrodynamic sizes of the formed aggregates. The CONTIN plots for $B_{800}V_{190}T_{380}$ and $B_{800}V_{190}T_{550}$ in acetone at 1 g/L and $\Theta = 90°$ are shown in Figure 2A, and plots of the decay rate, Γ, versus the square of the scattering vector, q^2, are shown in Figure 2B.

The micelles are very uniform, as shown by the unimodal CONTIN plots in Figure 2A. These aggregates can be considered to be almost monodisperse (PDI $\approx$ 0.02). The hydrodynamic radii, R_h, of both polymers (from the diffusion coefficients, slope of Figure 2B) and the corresponding polydispersities calculated via cumulant analysis at 90° measurement angle are shown in Table 2. Note that no significant change in the R_h was obtained for concentrations from 0.05 up to 5 g/L. The linearity of the decay rate plots, Γ versus q^2, and the lack of an intercept in Figure 2B indicates pure translational diffusion, which is typical of spherical particles.

Static Light Scattering. SLS experiments were performed in acetone ($0.1 \leq c \leq 1$ g/L) and analyzed using a Zimm plot.[31] The results are shown in Table 2. A representative Zimm plot is shown in Figure 3 for $B_{800}V_{190}T_{380}$ at four different concentrations.

The molecular weights of both micellar aggregates are comparable ($M_w = 2.38 \times 10^7$ g/mol for $B_{800}V_{190}T_{380}$ and 1.17×10^7 g/mol for $B_{800}V_{190}T_{550}$), resulting in a higher aggregation number of the BVT terpolymer with lower P*t*BMA molecular weight. This corresponds to theoretical expectations and results

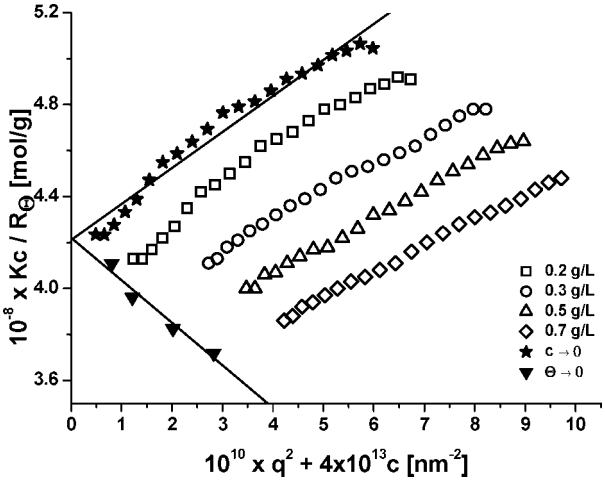

Figure 3. Zimm plot of $B_{800}V_{190}T_{380}$ in acetone.

of diblock copolymer micelles, where it was derived that $N_{agg} \approx N_A^2 N_B^{-0.8}$, where N_A and N_B correspond to the degrees of polymerization of the core- and corona-forming block of strongly segregating systems, respectively.[32] The degrees of aggregation, N_{agg}, were calculated using the known molecular weights of the precursors and are given in Table 2. A further elucidation of the structure can be achieved by evaluating the characteristic ratio, R_g/R_h. This ratio provides an indication about the shape of the scattering particle.[33] For hard spheres, the ratio is expected to be 0.775, whereas a ratio of 1.1 is expected for polymeric stars with a high arm number. In this particular case, the value for $B_{800}V_{190}T_{380}$ fits the hard spheres model, whereas the slightly higher value for the polymer with the longer methacrylate block might indicate a tendency toward a more starlike solution structure. In both cases, low negative values for the virial coefficient, A_2, are obtained, indicating that acetone is not a good solvent for the micelle. This is a known phenomenon of micellar solutions. The high aggregation numbers around 200 lead to a high segment density close to the micellar core, and hence few solvent molecules are present in between the single corona chains.[34]

To recapitulate, dynamic as well as static light scattering revealed that BVT terpolymers form almost monodisperse spherical micelles in acetone as a nonsolvent for polybutadiene.

Transmission Electron Microscopy. Typically, the specimens for TEM measurements were prepared through drop-coating from micellar solutions of approximately 0.1 g/L on carbon-coated gold grids. This concentration is above the critical aggregation concentration (cac), as indicated by DLS measurements. If not mentioned, the samples were not stained, and the contrast originates only from the different polymeric microcompartments. Although TEM is an elegant way to visualize the shape and the size of particles in the nanometer range, one has to be aware that the shape of particles may be affected by the drying procedure on the TEM grids. To confirm the obtained results, specimens were also prepared through freeze drying and spray coating from acetone for two examples. Unfortunately, we have been unable to perform cryo-TEM in acetone. Therefore, freeze drying is supposed to have the smallest influence on the micellar structure obtained on the TEM specimen. The obtained micelles are very uniform in size. No larger aggregates are present, as shown in Figure 4A,B for $B_{800}V_{190}T_{550}$ employing two different preparation methods.

Only a single micellar population is present. The image reveals uniformly dispersed objects with an average diameter of 40−50 nm, corresponding to the micellar core, which is subdivided into segregated domains. The central element (PB, gray) bears several black objects (P2VP, black), spherical in shape with an average diameter of 10−15 nm. For the polymers investigated in this work, numbers of three to six PVP spheres were found. The rather strong contrast originates from the difference in electron density between PB and P2VP. The multicompartmental character of the aggregates is unveiled in the enlargement in Figure 4C, whereas part D shows the proposed solution structure of the micellar aggregates. This type of micellar core is referred to as "spheres on sphere" or "raspberry-like".[18] The P*t*BMA corona is not visible because of its immediate degradation upon irradiation with the electron beam.

It remains puzzling that P2VP seems to be insoluble in acetone for our system. According to literature and our own experiments, P2VP homopolymer is soluble in acetone.[35] If homopolymers of comparable molecular weight are dissolved in acetone at a comparable concentration, then no aggregation is observed. For the BVT polymers, however, the formation of spherical, collapsed domains situated on the soft PB core seems to be more favorable. One tentative explanation may be the strong incompatibility between the first and the second block ($\chi_{BV} = 0.325$).[36] The strong driving force for minimization of the interface between PB and P2VP could hamper the formation of a continuous shell around the micellar core and therefore result in a further compartmentalization of the P2VP phase. A similar morphology was first described by Stadler et al. for the bulk morphology of polystyrene-*b*-polybutadiene-*b*-poly(methyl methacrylate) (SBM) triblock terpolymers with a certain composition.[37] Later, nanostructured aggregates like this SBM terpolymer were dispersed in a polymerizable matrix and were stabilized in that way for further examination.[38,39] Comparable micellar morphologies have been observed for mixtures of PS-*b*-P2VP-*b*-PEO block terpolymers with PAA in DMF.[40] Recently, Laschewsky et al. also reported on a linear poly(4-methyl-4-(4-vinylbenzyl)morpholin-4-ium chloride)-*b*-polystyrene-*b*-poly(pentafluorophenyl 4-vinylbenzyl ether) (PVBM-*b*-PS-*b*-PVBFP) triblock terpolymer which self-assembled into micelles with a similarly compartmentalized core in aqueous solution.[18] In their case, the two hydrophobic and insoluble blocks, one of them fluorinated, built the two different core domains.

In conclusion, TEM measurements show the formation of micelles with a very low polydispersity. Furthermore, first hints of a multicompartmental character of the micellar core are observed.

Cross-Linking. There is a significant interest in the stabilization of polymer micelles. In that way, their dynamic structure can be altered to facilitate the transfer of such aggregates into nonselective solvents or to stabilize them even below the critical micellar concentration.[41] Cross-linking of the core of the presented multicompartment micelles in acetone was performed via two different methods: "cold vulcanization" with S_2Cl_2, generating sulfur−sulfur bonds between neighboring double bonds of the polybutadiene compartment, or by applying a multifunctional acrylate (pentaerythrol tetraacrylate, PETA) as cross-linking agent and subsequent UV irradiation. The advantage of the latter is that the so-formed junctions between different polymer chains are almost irreversible and not, as for the cold vulcanization, prone to hydrolysis in acidic media. Both methods preferentially cross-link the 1,2-part of the polybutadiene segment. The content of 1,2-microstructure was measured via ^{1}H NMR to be around 86% for the BVT terpolymers, thus facilitating the cross-linking.[42] The pathway for the cross-linking procedure is depicted in Scheme 1.

Cross-Linking with S_2Cl_2. In the case of $B_{800}V_{190}T_{550}$, cross-linking was carried out with 1 equiv of S_2Cl_2 relative to the number of double bonds. The hydrodynamic radii of the initial

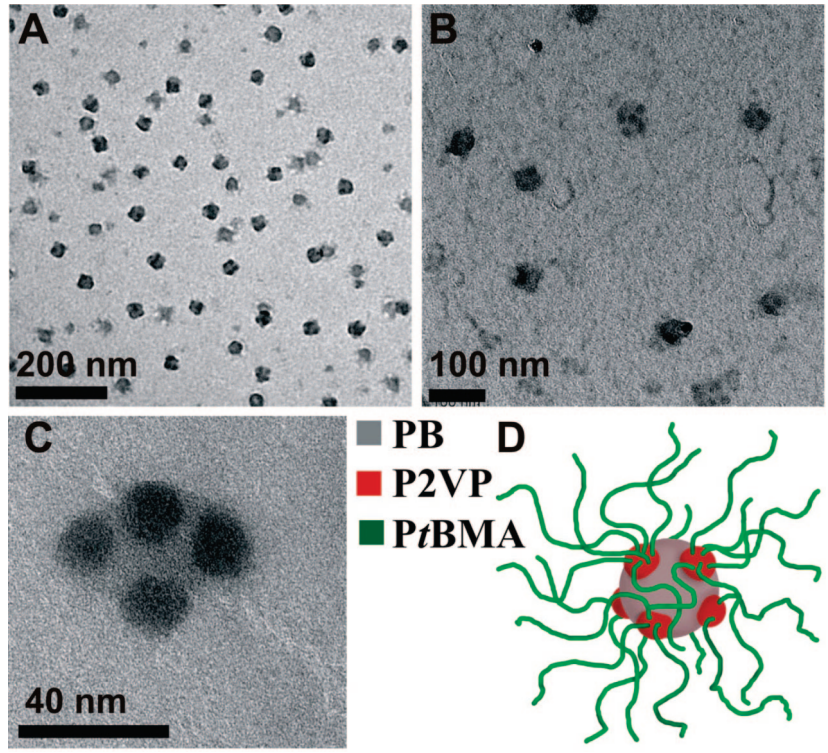

Figure 4. TEM images of multicompartment micelles from $B_{800}V_{190}T_{550}$ (A) drop-coated and (B) freeze dried from 0.1 g/L acetone onto carbon-coated gold TEM grids. (C) Single micelle at high magnification. (D) Proposed solution structure of the micelles.

Scheme 1. Cross-Linking Procedure for the PB Core of the Multicompartment Micelles via Two Different Methods: Cold Vulcanization with S_2Cl_2 and a Pentaerythrol Tetraacrylate

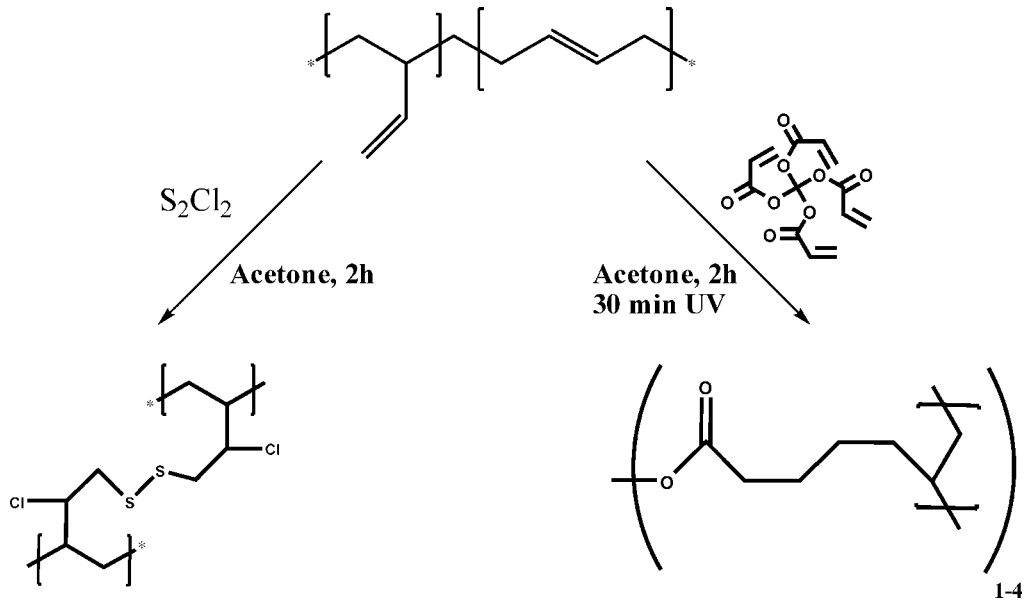

micelles in acetone (c = 1 g/L), the cross-linked micelles in acetone, and finally, after exchange of the solvent to THF are shown in Figure 5A.

After cross-linking, the hydrodynamic radii in acetone increase from 44 to about 49 nm. The CONTIN analysis still reveals only one size of micellar aggregates. Furthermore, cross-linking seemed to take place only within the micelles, and no intermicellar cross-linking occurs. Cumulant analysis at Θ = 90° results in a PDI of 0.031. It remains unclear why a significantly higher PDI is obtained after the cross-linking procedure. The increase in the hydrodynamic radius after cross-linking in acetone is due to the incorporation of the voluminous cross-linking agent, S_2Cl_2, into the micellar core. After transfer of the micellar solution into THF by dialysis, the size of the aggregates further increases to values of about 64 nm (PDI = 0.038). This indicates that the polybutadiene part of the core is still able to swell in THF, which is a nonselective solvent for all three blocks. However, the presence of only one population of aggregates, even in THF solution, is clear proof of the successfully performed cross-linking. The block terpolymer itself is molecularly soluble in THF.

To probe the effect of the amount of cross-linking agent and the reaction time on the size of the aggregates, $B_{800}V_{190}T_{380}$ was cross-linked with 1 and 5 equiv of S_2Cl_2 for 2 h and with 1

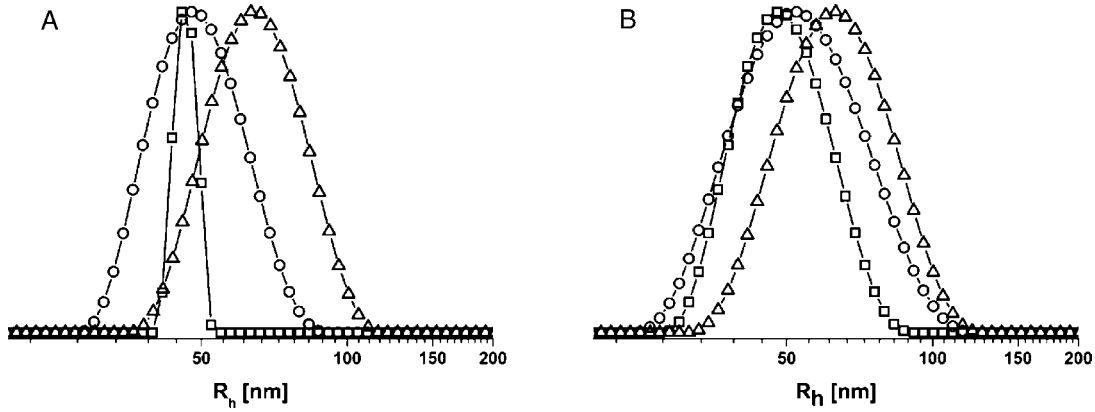

Figure 5. DLS CONTIN plots ($\theta = 90°$; $c = 1$ g/L, intensity-weighted) of micellar solutions: (A) $B_{800}V_{190}T_{550}$ in acetone (-□-, $\langle R_h \rangle_z = 44$ nm), after cross-linking of the polybutadiene core with 1 equiv of S_2Cl_2 (-○-,$\langle R_h \rangle_z = 49$ nm), and after transfer of the cross-linked micellar aggregates to THF through dialysis (-△-,$\langle R_h \rangle_z = 64$ nm); (B) $B_{800}V_{190}T_{380}$ in acetone after cross-linking with 1 equiv (-□-,$\langle R_h \rangle_z = 48$ nm) and 5 equiv (-○-,$\langle R_h \rangle_z = 53$ nm) of S_2Cl_2 for 2 h and 1 equiv (-△-,$\langle R_h \rangle_z = 64$ nm) for 96 h.

Table 3. Cross-Linking Efficiency of S_2Cl_2 for $B_{800}V_{190}T_{380}$ in Acetone

equiv S_2Cl_2[a]	reaction time (h)	insoluble material (%)[b]
1	2	9
2	2	42
5	2	65
1	96	46

[a] Relative to the amount of double bonds in PB. [b] Determined by ^{1}H NMR in THF-d_6.

equiv for 96 h. The results are shown in Figure 5B. The hydrodynamic radius before cross-linking is around 43 nm. For 1 equiv of cross-linking agent, the size of the micellar aggregates increases slightly to about 48 nm (PDI = 0.053). For 5 equiv of S_2Cl_2, the value for R_h increases to 53 nm (PDI = 0.064). With increasing concentration of S_2Cl_2, more incorporation takes place within the same reaction time. This indicates that the cross-linking is not completed after 2 h. If the reaction time is increased to 96 h, then the micelles show $R_h = 64$ nm afterward (PDI = 0.065). The cross-linking reaction proceeds very controlled because only one micellar population was obtained, and no larger aggregates could be detected via the CONTIN analysis. Also, here the PDI increases after the treatment with S_2Cl_2. To determine the actual amount of cross-linking, we removed the solvent and dissolved the residue in deuterated THF to perform ^{1}H NMR measurements. The ratio of the integral of the protons of the *tert*-butyl group ($\delta = 1.4$) was compared with the diminished 1,2-polybutadiene signals ($\delta = 4.8$) to determine the extent of cross-linking. The obtained results were cross-checked through Soxhlett extraction with THF for 48 h and are summarized in Table 3.

With increasing amount of cross-linking agent, the extent of cross-linking also increases. For 5 equiv of S_2Cl_2, the cross-linked polymer could not be dissolved in THF after evaporation of the acetone. Therefore, the acetone dispersion was mixed with deuterated *N*-methyl pyrrolidone (NMP), and acetone was evaporated. Table 3 also demonstrates that for a lower amount of S_2Cl_2, a longer reaction time is required to reach the same cross-linking efficiency.

Cross-Linking with Pentaerythrol Tetraacrylate. Poly(*tert*-butyl methacrylate) can be easily transformed into poly(methacrylic acid) by acidic treatment. With regard to the micellar aggregates presented here, this will generate an amphiphilic structure. To facilitate stable micellar solutions in aqueous media at different pH values, another method for the cross-linking of the core had to be found to avoid the hydrolysis of the sulfur−sulfur bonds in acidic media. Contrary to the above-discussed cold vulcanization technique, this multifunctional acrylate provides an efficient and

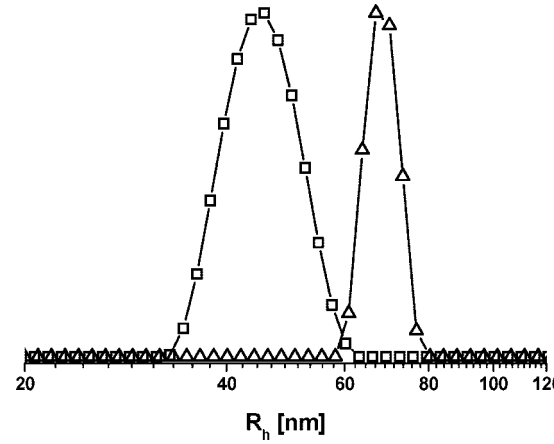

Figure 6. R_h of $B_{800}V_{190}T_{550}$ after cross-linking with 1 equiv of PETA in acetone (-□-,$\langle R_h \rangle_z = 46$ nm) and after transfer to dioxane (-△-,$\langle R_h \rangle_z = 67$ nm) ($c = 1$ g/L).

convenient way of pH-robust cross-linking junctions. Acetone micellar solutions of $B_{800}V_{190}T_{550}$ ($c = 1$ g/L) were mixed with defined solutions of PETA. The actual amount of cross-linking agent is given in equivalents of functional groups cross-linking agent with respect to the amount of reactive double bonds on the polymer chains in solution. After equilibration (24 h), the dispersions were exposed to UV light (300−400 nm) for 60 min. Subsequently, unreacted cross-linking agent was removed through dialysis. The hydrodynamic radii, R_h, of $B_{800}V_{190}T_{550}$ cross-linked with 1 equiv PETA and after subsequent transfer to dioxane are shown in Figure 6.

Initial R_h values for $B_{800}V_{190}T_{550}$ in acetone were 44 nm. After cross-linking with 1 equiv of PETA, basically the same values were obtained with 46 nm (PDI = 0.024). Surprisingly, in this case, the micellar core does not seem to increase significantly upon cross-linking. The amount of insoluble material was determined, as described for the cold vulcanization technique, and was 63% for 0.5 equiv and 67% for 1 equiv of cross-linking agent. Transfer to dioxane resulted again in larger aggregates with $\langle R_h \rangle_z = 67$ nm (PDI = 0.025), proving the successful cross-linking. According to the literature, PETA forms an interpenetrating network upon photopolymerization.[43,44] We suppose that this network forms junctions with the PB core (cf. Scheme 1). Without added PETA, UV irradiation of BVT block terpolymer micelles in acetone did not lead to cross-linked aggregates.

In summary, the presented multicompartment micelles exhibited single micellar populations in all cases demonstrated

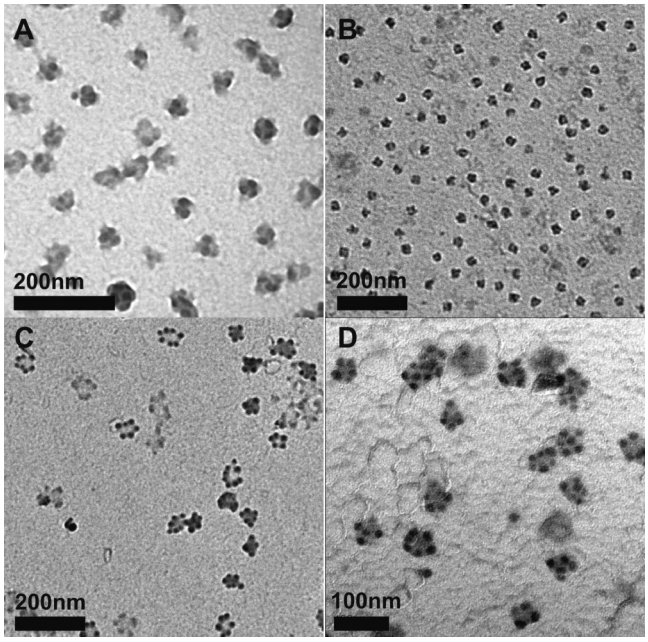

Figure 7. TEM images of micelles drop-coated from 0.1 g/L dispersion in (A,B) acetone and (C,D) THF. (A) $B_{800}V_{190}T_{550}$ after cross-linking with S_2Cl_2; (B) $B_{800}V_{190}T_{550}$ after cross-linking with PETA; (C) $B_{800}V_{190}T_{550}$ dispersion of part C after dialysis to THF; (D) $B_{800}V_{190}T_{550}$ dispersion of part A after staining with iodine.

here. To assess structure and shape of the micelles after the various treatments, the micellar solutions were drop-coated onto carbon-coated TEM grids. TEM images of different dispersions are shown in Figure 7.

Figure 7A shows $B_{800}V_{190}T_{550}$ multicompartment micelles after cross-linking with 1 equiv of S_2Cl_2 from acetone. The compartmentalization of the core is still present, the contrast just decreased slightly. This could be explained by the incorporation of sulfur and chlorine into the polybutadiene compartment and therefore the convergence of the electron density for the two core-forming compartments. As already indicated by the DLS measurements in Figure 5A, the size of the aggregates slightly increases. In Figure B, micelles from $B_{800}V_{190}T_{550}$ after cross-linking of the core with 1 equiv PETA are presented. Again, size and shape seem to be conserved. Figure 6C represents micelles from $B_{800}V_{190}T_{550}$ after cross-linking with 1 equiv of S_2Cl_2 and subsequent transfer of the aggregates into THF as a nonselective solvent, which is then able to swell the partially cross-linked core, as already shown by means of DLS in Figure 5A. Figure D exhibits $B_{800}V_{190}T_{550}$ multicompartment micelles after cross-linking with S_2Cl_2 and subsequent staining with iodine. I_2 preferentially enhances electron density in the poly(2-vinyl pyridine) compartment. This treatment makes the two compartments of the micellar core even more distinguishable from each other. A sharp borderline can be clearly seen between the gray polybutadiene and the black poly(2-vinyl pyridine). Staining with OsO_4, which reacts with the 1,4-polybutadiene units,[45] has also been carried out. Unfortunately, this treatment did not give any further insight.

In conclusion, the multicompartmental character of the micellar aggregates is fully preserved after cross-linking with either S_2Cl_2 or PETA. The cross-linking success is proven through the successful transfer of the micelles into THF or dioxane. Iodine staining was successfully employed to enhance the phase contrast between the two core-forming departments in TEM measurements.

Cryogenic Transmission Electron Microscopy. Cryo-TEM can be employed to explore the micellar structure in situ without any drying effects.[46] Most of the work on cryo-TEM reported in the literature has been performed in water. In this work, either THF or dioxane was taken as solvent. We have recently shown that cryo-TEM in THF can successfully be used to explore complex aggregation patterns.[47] The concentration of the samples investigated varied from 0.1 to 0.7 g/L. A general effect across all samples investigated is that instead of single micelles, continuous structures could be observed. This is shown in Figure 8 for S_2Cl_2 core-cross-linked micelles of $B_{800}V_{190}T_{550}$.

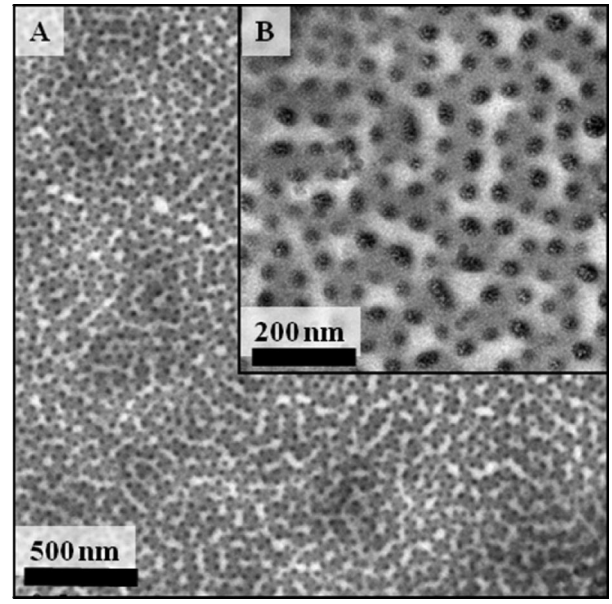

Figure 8. Cryo-TEM images of $B_{800}V_{190}T_{550}$ in THF after cross-linking of the polybutadiene core with 1 equiv of S_2Cl_2 in acetone and subsequent transfer of the aggregates into THF through dialysis: (A) overview and (B) enlargement; $c = 0.5$ g/L.

Figure 8A,B shows an overview over an area with the continuous structure and an enlargement, respectively. Both images were taken from vitrified THF solutions at a concentration of 0.5 g/L. Similar results could be obtained in the concentration range from 0.1 to 0.7 g/L. Basically, the multicompartmental character can be confirmed. Grey elongated structures bearing black dots are visible. Clearly, the black parts consist of poly(2-vinyl pyridine), which is the material with the highest electron density. The grayish compartments resemble the cross-linked polybutadiene, and the light parts in between are poly(*tert*-butyl methacrylate), which is well-soluble and swollen with THF. In this particular case, electron density in the polybutadiene compartment is enhanced through the cross-linking step and therefore the incorporation of sulfur and chlorine atoms. The observed vermicular structures could again be formed because of the strong incompatibility between polybutadiene and poly(2-vinyl pyridine).[36] The foremost random distribution of length and orientation of the elongated structures could be the result of interface minimization. Alongside the vermicular objects, the poly(2-vinyl pyridine) compartments are always situated in a "zigzag" manner and are never directly opposite. The formation of continuous structures could be explained through the evaporation of some solvent during the sample preparation and hence an increase in the sample concentration. It is noteworthy that the structures appear to be somewhat larger in cryogenic TEM measurements, again leading to the conclusion that the partially cross-linked micellar cores are still able to swell in THF to a certain extent.

Figure 9 shows an image taken from a vitrified micellar solution of $B_{800}V_{190}T_{550}$ micelles after "cold-vulcanization" and transfer into dioxane at a concentration of 0.1 g/L. For this specimen, similar aggregates were found but are not depicted

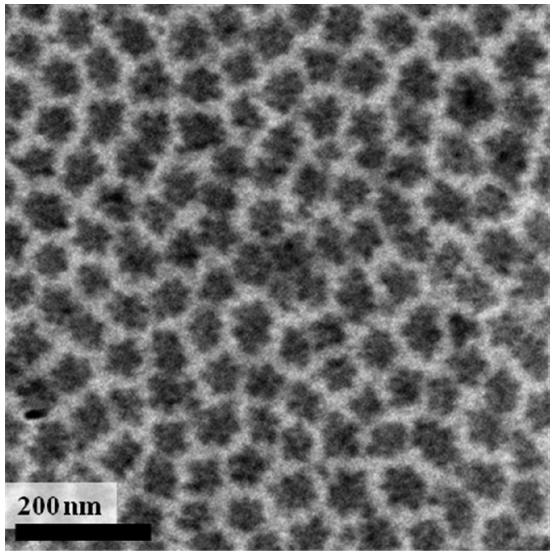

Figure 9. Cryo-TEM images of $B_{800}V_{190}T_{550}$ in dioxane after cross-linking of the polybutadiene core with 1 equiv of S_2Cl_2 in acetone and subsequent transfer of the aggregates into dioxane ($c = 0.2$ g/L).

here. Instead, Figure 9 presents single micellar aggregates. Coexistence of both structures was found over the whole specimen. Although the contrast is worse than that in Figure 8, the further compartmentalized core of the micelles can be visualized. The size shows an increase to about 60−70 nm per micellar core. That again can be explained through swelling of the partially cross-linked polybutadiene in the solvent. Some of the assemblies seem to merge, especially in the upper right corner of Figure 9. In that way, this cryo-TEM image may resemble the transition from single multicompartment micelles to the previously discussed continuous structures.

In conclusion, the cryo-TEM investigations show that the multicompartment micelles exist as single aggregates in dioxane and that the solvent is able to swell the partially cross-linked core.

Conclusions

This work shows for the first time that multicompartment micelles from ABC triblock terpolymers, $B_{800}V_{190}T_{380}$ and $B_{800}V_{190}T_{550}$, can be easily prepared when they are dissolved in acetone. In contrast with other works within this field, neither complex polymer architecture nor extraordinary monomers had to be employed for the formation of a further compartmentalized micellar core; all three monomers are common, cheap, and available in large amounts. The convenient synthesis pathway allows the preparation of the triblock terpolymers on a large scale. The structure of the aggregates could be assessed via TEM and cryo-TEM measurements. The uniformity of the formed aggregates was proven with several dynamic and static light scattering experiments. The cross-linking of the polybutadiene compartment with two inherently different methods was not shown to alter the structure of the micelles. In the case of the cold vulcanization pathway, the effect of the amount of cross-linking agent and reaction time has been investigated. For the cross-linking with a multifunctional acrylate, two main differences could be observed: first, the micellar core does not seem to increase through the incorporation of the pentaerythrol tetraacrylate, which definitely happened for S_2Cl_2, and second, the newly formed junctions between polymer chains are supposed to be stable with respect to the hydrolysis of the ester moiety of the poly(*tert*-butyl methacrylate) compartment and the transfer of the micelles into aqueous media at different pH values. The latter will be the subject of further research. Cross-linking was proven to be successful through the transfer of the aggregates into nonselective solvents, THF, and dioxane.

Acknowledgment. We thank VolkswagenStiftung for financial support. Special thanks also goes to all of the people who contributed to this work, in particular, Dr. Markus Burkhardt for discussions and Dr. Holger Schmalz and Denise Danz for help with the polymer synthesis.

References and Notes

(1) Ringsdorf, H.; Lehman, P.; Weberskirch, R. *Book of Abstracts, 217th ACS National Meeting*; American Chemical Society: Washington, DC, 1999.
(2) Lutz, J.-F.; Laschewsky, A. *Macromol. Chem. Phys.* **2005**, *206*, 813–817.
(3) Li, Z.; Hillmyer, M. A.; Lodge, T. P. *Macromolecules* **2006**, *39*, 765–771.
(4) Stahler, K.; Selb, J.; Barthelemy, P.; Pucci, B.; Candau, F. *Langmuir* **1998**, *14*, 4765–4775.
(5) Stahler, K.; Selb, J.; Candau, F. *Langmuir* **1999**, *15*, 7565–7576.
(6) Kotzev, A.; Laschewsky, A.; Adriaensens, P.; Gelan, J. *Macromolecules* **2002**, *35*, 1091–1101.
(7) Szczubialka, K.; Moczek, L.; Goliszek, A.; Nowakowska, M.; Kotzev, A.; Laschewsky, A. *J. Fluorine Chem.* **2005**, *126*, 1409–1418.
(8) Lodge, T.; Rasdal, A.; Li, Z.; Hillmyer, M. A. *J. Am. Chem. Soc.* **2005**, *127*, 17608–17609.
(9) Underhill, R. S.; Liu, G. *Chem. Mater.* **2000**, *12*, 2082–2091.
(10) Fustin, C. A.; Abetz, V.; Gohy, J. F. *Eur. Phys. J. E* **2005**, *16*, 291–302.
(11) Zheng, R.; Liu, G.; Yan, X. *J. Am. Chem. Soc.* **2005**, *127*, 15358–15359.
(12) Patrickios, C. S.; Forder, C.; Armes, S. P.; Billingham, N. C. *J. Polym. Sci., Part A: Polym. Chem.* **1997**, *35*, 1181.
(13) Kriz, J.; Massar, B.; Plestil, J.; Tuzar, Z.; Pospisil, H.; Doskociloca, D. *Macromolecules* **1998**, *31*, 41.
(14) Chen, W. Y.; Alexandridis, P.; Su, C. K.; Patrickios, C. S.; Hertler, W. R.; Hatton, T. A. *Macromolecules* **1995**, *28*, 8604.
(15) Yu, G. E.; Eisenberg, A. *Macromolecules* **1998**, *31*, 5546–5549.
(16) Stewart, S.; Liu, G. *Chem. Mater.* **1999**, *11*, 1048.
(17) Stähler, K.; Selb, J.; Candau, F. *Mater. Sci. Eng., C* **1999**, *10*, 171–178.
(18) Kubowicz, S.; Baussard, J.-F.; Lutz, J.-F.; Thünemann, A.; Berlepsch, H. v.; Laschewsky, A. *Angew. Chem. Int. Ed.* **2005**, *44*, 5262–5265.
(19) Thünemann, A.; Kubowicz, S.; Berlepsch, H. v.; Möhwald, H. *Langmuir* **2006**, *22*, 2506–2510.
(20) Li, Z.; Hillmyer, M. A.; Lodge, T. *Langmuir* **2006**, *22*, 9409–9417.
(21) Li, Z.; Kesselman, E.; Talmon, Y.; Hillmyer, M. A.; Lodge, T. P. *Science* **2004**, *306*, 98–101.
(22) Saito, N.; Liu, C.; Lodge, T. P.; Hillmyer, M. A. *Macromolecules* **2008**, *41*, 8815–8822.
(23) Mao, J.; Ni, P.; Mai, Y.; Yan, D. *Langmuir* **2007**, *23*, 5127–5134.
(24) Dormidontova, E. E.; Khokhlov, A. R. *Macromolecules* **1997**, *30*, 1980–1991.
(25) Chou, S.-H.; Tsai, H.-K.; Sheng, Y.-J. *J. Chem. Phys.* **2006**, *125*, 194903.
(26) Zhong, C.; Liu, D. *Macromol. Theory Simul.* **2007**, *16*, 141–157.
(27) Ma, Z.; Jiang, W. *J. Polym. Sci., Part B: Polym. Phys.* **2009**, *47*, 484–492.
(28) Freyss, D.; Rempp, P.; Benoit, H. *Polym. Lett.* **1964**, *2*, 217.
(29) Quirk, R. P.; Yoo, T.; Lee, Y.; Kim, J.; Lee, B. *Adv. Polym. Sci.* **2000**, *153*, 67–106.
(30) David, R. L. *CRC Handbook of Chemistry and Physics*, 81st ed.; CRC Press: Boca Raton, FL, 2000.
(31) Zimm, B. H. *J. Chem. Phys.* **1948**, *16*, 1099.
(32) Förster, S.; Zisenis, M.; Wenz, E.; Antonietti, M. *J. Chem. Phys.* **1996**, *104*, 9956–9970.
(33) Burchard, W. *Adv. Polym. Sci.* **1999**, *143*, 113–194.
(34) Erhardt, R.; Boker, A.; Zettl, H.; Kaya, H.; Pyckhout-Hintzen, W.; Krausch, G.; Abetz, V.; Mueller, A. H. E. *Macromolecules* **2001**, *34*, 1069–1075.
(35) Brandrup, J.; Immergut, E. H.; Grulke, E. A. *Polymer Handbook*, 4th ed.; John Wiley & Sons: New York, 1999.
(36) Barton, A. F. *CRC Handbook of Polymer Liquid Interaction Parameters and Solubility Parameters*; CRC Press: Boca Raton, FL, 1990.
(37) Breiner, U.; Krappe, U.; Jakob, T.; Abetz, V.; Stadler, R. *Polym. Bull.* **1998**, *40*, 219.
(38) Ritzenthaler, S.; Court, F.; David, L.; Girard-Reydet, E.; Leibler, L.; Pascault, J. P. *Macromolecules* **2002**, *35*, 6245.
(39) Ritzenthaler, S.; Court, F.; Girard-Reydet, E.; Leibler, L.; Pascault, J. P. *Macromolecules* **2003**, *36*, 118.

(40) Gohy, J. F.; Khousakoun, E.; Willet, N.; Varshney, S. K.; Jérôme, R. *Macromol. Rapid Commun.* **2004**, *25*, 1536–1539.
(41) O'Reilly, R. K.; Hawker, C.; Wooley, K. L. *Chem. Soc. Rev.* **2006**, *35*, 1068–1083.
(42) Hsieh, H. L.; Quirk, R. P. *Anionic Polymerization: Principles and Practical Applications*; Marcel Dekker: New York, 1996.
(43) Petrov, P.; Bozukov, M.; Tsvetanov, C. B. *J. Mater. Chem.* **2005**, *15*, 1481–1486.
(44) Petrov, P.; Yuan, J.; Yoncheva, K.; Müller, A. H. E.; Tsvetanov, C. B. *J. Phys. Chem. B* **2008**, *112*, 8879–8883.
(45) Kato, K. *J. Polym. Sci., Polym. Lett. Ed.* **1966**, *4*, 35.
(46) Adrian, M.; Dubochet, J.; Lepault, J.; McDowall, A. W. *Nature (London)* **1984**, *32*, 308.
(47) Walther, A.; Andre, X.; Drechsler, M.; Abetz, V.; Muller, A. H. E. *J. Am. Chem. Soc.* **2007**, *129*, 6187–6198.

MA9002424